Feedforward control for SPMSM with Final-State Control Based on Voltage Limit Circle with Transient Term

Takayuki Miyajima
The University of Tokyo
Kashiwa, Chiba, Japan
miya@fujilab.k.u-tokyo.ac.jp

Hiroshi Fujimoto
The University of Tokyo
Kashiwa, Chiba, Japan
fujimoto@k.u-tokyo.ac.jp

Masami Fujitsuna
DENSO CORPORATION
Kariya, Aichi, Japan
MASAMI_FUJITSUNA@denso.co.jp

***Abstract*— SPMSMs (Surface Permanent Magnet Synchronous Motors) are employed for many industrial applications. SPMSM drive systems should achieve quick torque response and wide operating range. For quick current response, authors proposed final-state control considering voltage limit. Final-state control drives an initial state to a final state with feedforward input during finite time. The proposed method achieved quick current control in field-weakening region but inverse response of q-axis current was caused. In this paper, a new feedforward control method which improves current response is proposed. Simulations and experiments are performed to compare two types of feedforward control method. In addition, current response under voltage limit is analyzed by the voltage limit circle of SPMSM with transient term.**

I. INTRODUCTION

Permanent magnet synchronous motors (PMSMs) are widely employed in many industries because of high efficiency, high power density. Surface PMSMs (SPMSMs) are used for machine tool and electric power steering (EPS). In these applications, SPMSM drive systems are demanded high-speed operation and quick torque response but output voltage is limited. Especially, in the EPS system, the dc voltage supply is battery. Therefore, to achieve high performance is difficult due to low output voltage. In addition, from view point of torque ripple, the overmodulation range of inverter is not unavailable.

In the SPMSM drive systems, field-weakening control is applied to expand the operating range. However, in field-weakening region, voltage amplitude is reached the voltage limit. Therefore, the manipulated variable is voltage phase only. General methods determine d-axis and q-axis voltage independently but it cannot operate voltage phase directly. Thus, quick current response cannot be achieved and control method which can operate voltage phase directly is required.

Many methods for qucik torque response under the voltage limit had been studied. Methods which operate voltage phase with the voltage limiter [1][2], control torque and modulation index by torque loop [3][4], and operate voltage phase directly by feedback (FB) controller [5][6] were proposed. However, for quicker response, feedforward (FF) controller should be used.

For the quickest current response under voltage limit, authors proposed a final-state control [7] for SPMSM considering voltage limit [8]. Conventional final-state controls featured single-input single-output system. On the other hand, this proposed method controls SPMSM of two-input two-output system. SPMSM control under voltage limit can be described as the programming problem whose evolution function and constraint function are quadratic function and quadratic inequality in form of linear matrix inequality (LMI), respectively. The quickest current response was realized by FF input (FSC input) which is obtained by solving these LMIs. In this paper, for improving current response, a new FSC input is proposed. In addition, this paper analyzes FSC input by voltage limit circle with transient term.

II. MODEL AND DISCRETIZATION

A. dq Model of SPMSM

The voltage equation of SPMSM in dq-axis is represented in the form of state equation as $\boldsymbol{y} = \boldsymbol{x} = [i_d \quad i_q]^T$ and $\boldsymbol{u} = [v_d \quad v_q]^T$ by

$$\dot{\boldsymbol{x}}(t) = \boldsymbol{A_c}(\omega_e)\boldsymbol{x}(t) + \boldsymbol{B_c}\left\{\boldsymbol{u}(t) - \begin{bmatrix} 0 & \omega_e K_e \end{bmatrix}^T\right\}, \tag{1}$$

$$\boldsymbol{y}(t) = \boldsymbol{C_c}\boldsymbol{x}(t), \tag{2}$$

$$\left[\begin{array}{c|c} \boldsymbol{A_c}(\omega_e) & \boldsymbol{B_c} \\ \hline \boldsymbol{C_c} & \boldsymbol{0} \end{array}\right] := \left[\begin{array}{cc|cc} -\frac{R}{L} & \omega_e & \frac{1}{L} & 0 \\ -\omega_e & -\frac{R}{L} & 0 & \frac{1}{L} \\ \hline \multicolumn{2}{c|}{\boldsymbol{I}} & \multicolumn{2}{c}{\boldsymbol{0}} \end{array}\right], \tag{3}$$

where $v_{d,\,q}$ are the d-axis and q-axis voltage, R is the stator winding resistance, L is the inductance, ω_e is the electric angular velocity, $i_{d,\,q}$ are the d-axis and q-axis current, and K_e is the back EMF constant.

The motor torque T is given by

$$T = K_{mt} i_q, \tag{4}$$

where $K_{mt} := PK_e$ and P is the number of pole pairs. In this paper, 2-phase/3-phase transform is absolute transformation.

B. Discretization Based on PWM Hold

In order to discretize a plant, a zero-order hold is generally applied. However, in the case of single-phase inverter, it cannot output arbitrary voltage but only 0 or $\pm E$ (E is the dc-bus voltage of single-phase inverter). Therefore, in order to control instantaneous values precisely, the zero-order hold is not suitable. When the pulse is allocated in the center of control period T_u, the plant in inverter drive system can be discretized as follows [11].

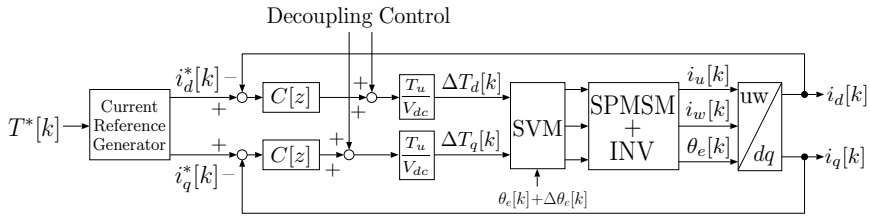

Fig. 1. Conventional method

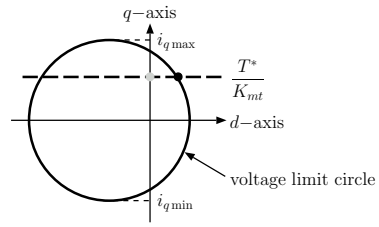

Fig. 2. Intersection point of voltage limit circle with constant torque line

A continuous-time state equation of a plant is given by

$$\dot{\boldsymbol{x}}(t) = \boldsymbol{A}_c\boldsymbol{x}(t) + \boldsymbol{B}_c\boldsymbol{u}(t),\ \boldsymbol{y}(t) = \boldsymbol{C}_c\boldsymbol{x}(t). \tag{5}$$

The precise discrete model in which the input is the ON time $\Delta\boldsymbol{T}[k]$ is obtained as

$$\boldsymbol{x}[k+1] = \boldsymbol{A}_s\boldsymbol{x}[k] + \boldsymbol{B}_s\Delta\boldsymbol{T}[k],\ \boldsymbol{y}[k] = \boldsymbol{C}_s\boldsymbol{x}[k], \tag{6}$$

$$\boldsymbol{A}_s := e^{\boldsymbol{A}_c T_u},\ \boldsymbol{B}_s := e^{\boldsymbol{A}_c T_u/2}\boldsymbol{B}_c E,\ \boldsymbol{C}_s := \boldsymbol{C}_c. \tag{7}$$

In derivation of (6) and (7), the voltage amplitude is considered $+E$ only. Therefore, if $\Delta\boldsymbol{T}[k]$ is negative, the voltage amplitude is $-E$.

C. PWM Hold Model of SPMSM

(1) is discretized based on PWM hold. Here, it is assumed that the speed variation during one control period can be neglected. Hence, the back EMF $\omega_e K_e$ can be presumed as the zero-order hold. Therefore, the PWM hold model of SPMSM is designed as $E = V_{dc}$ in (5) as follows:

$$\boldsymbol{x}[k+1] = \boldsymbol{A}_s(\omega_e)\boldsymbol{x}[k] + \boldsymbol{B}_s(\omega_e)\Delta\boldsymbol{T}[k] - \boldsymbol{B}_{s2}(\omega_e)\begin{bmatrix}0 & \omega_e K_e\end{bmatrix}^T, \tag{8}$$

$$\boldsymbol{y}[k] = \boldsymbol{C}_s\boldsymbol{x}[k], \tag{9}$$

$$\boldsymbol{A}_s(\omega_e) := e^{\boldsymbol{A}_c(\omega_e)T_u},\ \boldsymbol{B}_s(\omega_e) := e^{\boldsymbol{A}_c(\omega_e)\frac{T_u}{2}}\boldsymbol{B}_c V_{dc},$$

$$\boldsymbol{B}_{s2}(\omega_e) := \boldsymbol{A}_c^{-1}(\omega_e)\left(e^{\boldsymbol{A}_c(\omega_e)T_u} - \boldsymbol{I}\right)\boldsymbol{B}_c, \tag{10}$$

where V_{dc} is the dc-bus voltage of three-phase inverter, $\Delta\boldsymbol{T} = [\Delta T_d \quad \Delta T_q]^T$, and $\Delta T_{d,\,q}$ are the d-axis and q-axis ON time. $\boldsymbol{A}_s(\omega_e)$, $\boldsymbol{B}_s(\omega_e)$, and $\boldsymbol{B}_{s2}(\omega_e)$ are functions of ω_e. Thus, these functions should be calculated again when ω_e is changed.

Here, input of three-phase can be generated based on space vector modulation (SVM) [12].

III. Control system design

A. Conventional method

Fig. 1 shows the block diagram of the conventional method. The decoupling control which is given by (11), (12) is applied.

$$v_d^{ref}[k] = v_d'^{ref}[k] - \omega_e[k]Li_q[k] \tag{11}$$

$$v_q^{ref}[k] = v_q'^{ref}[k] + \omega_e[k](Li_d[k] + K_e) \tag{12}$$

The current PI controller is designed with pole-zero cancellation as follows:

$$C(s) = \frac{Ls+R}{\tau s}, \quad \tau = 10T_u \tag{13}$$

By discretizing (13), $C[z]$ is obtained by Tustin transformation with control period T_u. Here, if $V_a := \sqrt{v_d^2 + v_q^2} > V_{\max}$ (V_a is the voltage amplitude and $V_{\max} := \sqrt{\frac{3}{2}}\frac{V_{dc}}{\sqrt{3}}$ is the maximum value of voltage amplitude.), the integrator of $C[z]$ is stopped.

The current reference generator makes d-axis and q-axis current references i_d^* and i_q^* from torque reference T^*. It selects the intersection point of the voltage limit circle with the constant torque line as Fig. 2. The generation of current references is represented by

$$i_d^*[k] = \frac{-\omega_e^2 K_e L}{R^2 + \omega_e^2 L^2} + \sqrt{(i_{q\max} - i_q^*)(i_q^* - i_{q\min})}, \tag{14}$$

$$i_q^*[k] = \begin{cases} i_{q\max} & \text{if } T^*[k] > K_{mt} i_{q\max} \\ i_{q\min} & \text{elseif } T^*[k] < K_{mt} i_{q\min} \\ \frac{T^*[k]}{K_{mt}} & \text{otherwise} \end{cases}, \tag{15}$$

$$i_{q\max} := -\frac{\omega_e K_e R - V_a\sqrt{R^2 + \omega_e^2 L^2}}{R^2 + \omega_e^2 L^2}, \tag{16}$$

$$i_{q\min} := -\frac{\omega_e K_e R + V_a\sqrt{R^2 + \omega_e^2 L^2}}{R^2 + \omega_e^2 L^2}. \tag{17}$$

If d-axis current reference is selected to strengthen field flux, $i_d^*[k] = 0$.

$\Delta\theta_e (= 0.5\omega_e T_u)$ is added to θ_e in the dq/2-phase transform for sampling error compensation [13]. The ON time limit in SVM is described by

$$\Delta\tilde{\boldsymbol{T}}[k] = \begin{cases} \frac{\Delta\boldsymbol{T}[k]}{|\Delta\boldsymbol{T}[k]|}\Delta T_{\max} & \text{if } |\Delta\boldsymbol{T}[k]| > \Delta T_{\max} \\ \Delta\boldsymbol{T}[k] & \text{otherwise} \end{cases}, \tag{18}$$

where $\Delta T_{\max}\left(:= \sqrt{\frac{3}{2}}\frac{T_u}{\sqrt{3}}\right)$ is the maximum value of dq-axis ON time vector amplitude and $\Delta\tilde{\boldsymbol{T}}[k]$ is the limiter output. In this paper, all limiters are calculated in the same way as (18).

B. Proposed method

Fig. 3 and 4 show the block diagrams of the proposed method and FF controller $\boldsymbol{C}_1[z]$, respectively. The proposed method consists of the 2-DOF control system and has two types of FF controllers.

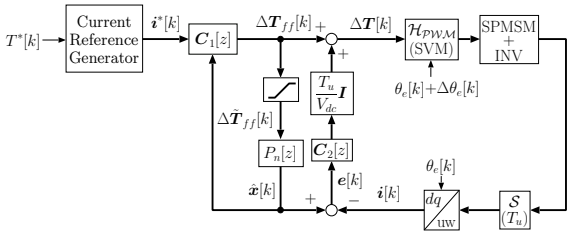

Fig. 3. Proposed method

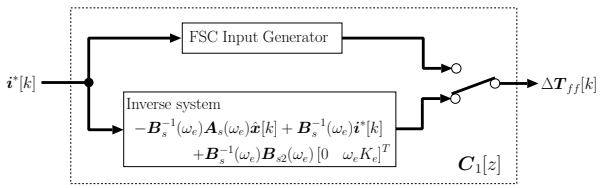

Fig. 4. Feedforward controller of proposed method

The inverse system of (8) is derived as follows:

$$\begin{aligned}\Delta\boldsymbol{T}_{ff}[k] = &-\boldsymbol{B}_s^{-1}(\omega_e)\boldsymbol{A}_s(\omega_e)\hat{\boldsymbol{x}}[k]+\boldsymbol{B}_s^{-1}(\omega_e)\boldsymbol{x}_d[k+1]\\ &+\boldsymbol{B}_s^{-1}(\omega_e)\boldsymbol{B}_{s2}(\omega_e)\begin{bmatrix}0 & \omega_e K_e\end{bmatrix}^T \end{aligned} \tag{19}$$

The inverse system used as a feedforward controller assures perfect tracking if the plant is nominal and the feedforword input is not limited. $\hat{\boldsymbol{x}}[k] := [\hat{i}_d[k] \quad \hat{i}_q[k]]^T$ is the nominal ouput which takes the input limit into consideration.

If the feedforward input from the inverse system is not limited, the inverse system is used as a feedforward controller. On the other hand, if the feedforward input from the inverse system is limited, the feedforward input is recalculated with FSC input generator to achieve quick current response. Here, the proposed method switches the type of feedforward controller but the inverse system is equal to final-state control whose prescribe time interval is one. Therefore, the switch does not make unstable.

The FB controller $\boldsymbol{C}_2[z]$ suppresses the current error $\boldsymbol{e}[k]$ between $\hat{\boldsymbol{x}}[k]$ and $\hat{\boldsymbol{x}}[k]$. Here, $\boldsymbol{C}_2[z]$ is the same as the FB controller of conventional method. However, in the proposed method, anti-windup control is not necessary because $\hat{\boldsymbol{x}}[k]$ considers the input limit.

1) Proposed method 1[8]: Final-state control drives an initial state to a final state by prescribed time interval. Here, final-state control considering voltage limit is expressed as a programming program whose evaluation function and constraint functions are quadratic function and quadratic inequality in the form of LMI, respectively. The FF input called FSC input is generated by solving these LMIs.

From PWM hold model of SPMSM, a final state $\boldsymbol{x}[N]$ is represented with an initial state $\boldsymbol{x}[0]$ as follows:

$$\boldsymbol{Y} = \boldsymbol{\Sigma}\boldsymbol{U} \tag{20}$$

$$\boldsymbol{Y} := \boldsymbol{x}[N] - \boldsymbol{A}_s^N\boldsymbol{x}[0] - \boldsymbol{\Sigma}_2\boldsymbol{U}_{EMF} \tag{21}$$

$$\boldsymbol{\Sigma} := \begin{bmatrix}\boldsymbol{A}_s^{N-1}\boldsymbol{B}_s & \boldsymbol{A}_s^{N-2}\boldsymbol{B}_s & \cdots & \boldsymbol{B}_s\end{bmatrix} \tag{22}$$

$$\boldsymbol{\Sigma}_2 := \begin{bmatrix}\boldsymbol{A}_s^{N-1}\boldsymbol{B}_{s2} & \boldsymbol{A}_s^{N-2}\boldsymbol{B}_{s2} & \cdots & \boldsymbol{B}_{s2}\end{bmatrix} \tag{23}$$

$$\boldsymbol{U} := \begin{bmatrix}\Delta\boldsymbol{T}^T[0]\ \Delta\boldsymbol{T}^T[1]\cdots\Delta\boldsymbol{T}^T[N-1]\end{bmatrix}^T \tag{24}$$

$$\boldsymbol{U}_{EMF} := -\omega_e K_e\begin{bmatrix}0 & 1 & \cdots & 0 & 1\end{bmatrix}^T \tag{25}$$

Here, it is assumed that ω_e is constant in this derivation.

The FF input series $\boldsymbol{U}$ which satisfies (20) is not determined uniquely. Thereupon, the square sum of the current error is minimized. The evaluation function J is represented by

$$J = \boldsymbol{E}^T\boldsymbol{Q}\boldsymbol{E}, \quad \boldsymbol{Q} > 0, \tag{26}$$

$$\boldsymbol{E} := [\boldsymbol{e}[1]^T \ \ \boldsymbol{e}[2]^T\cdots\boldsymbol{e}[N]^T]^T, \tag{27}$$

$$\boldsymbol{e}[k] := \boldsymbol{i}^* - \boldsymbol{x}[k] = \begin{bmatrix}i_d^* & i_q^*\end{bmatrix}^T - \boldsymbol{x}[k], \tag{28}$$

$$\boldsymbol{E} := \boldsymbol{I}^* - \boldsymbol{A}\boldsymbol{x}[0] - \boldsymbol{B}\boldsymbol{U} - \boldsymbol{B}_2\boldsymbol{U}_{EMF}, \tag{29}$$

$$\boldsymbol{A} := \begin{bmatrix}\boldsymbol{A}_s & \boldsymbol{A}_s^2 & \cdots\boldsymbol{A}_s^N\end{bmatrix}^T, \tag{30}$$

$$\boldsymbol{B} := \begin{bmatrix}\boldsymbol{B}_s & 0 & \cdots & 0\\ \boldsymbol{A}_s\boldsymbol{B}_s & \boldsymbol{B}_s & \cdots & 0\\ \vdots & \vdots & \ddots & \vdots\\ \boldsymbol{A}_s^{N-1}\boldsymbol{B}_s & \boldsymbol{A}_d^{N-2}\boldsymbol{B}_s & \cdots & \boldsymbol{B}_s\end{bmatrix}, \tag{31}$$

$$\boldsymbol{B}_2 := \begin{bmatrix}\boldsymbol{B}_{s2} & 0 & \cdots & 0\\ \boldsymbol{A}_s\boldsymbol{B}_{s2} & \boldsymbol{B}_{s2} & \cdots & 0\\ \vdots & \vdots & \ddots & \vdots\\ \boldsymbol{A}_s^{N-1}\boldsymbol{B}_{s2} & \boldsymbol{A}_s^{N-2}\boldsymbol{B}_{s2} & \cdots & \boldsymbol{B}_{s2}\end{bmatrix}, \tag{32}$$

$$\boldsymbol{I}^* := \begin{bmatrix}(\boldsymbol{i}^*)^T & (\boldsymbol{i}^*)^T\cdots(\boldsymbol{i}^*)^T\end{bmatrix}^T. \tag{33}$$

Moreover, (8) is controllable. Thus, $\boldsymbol{\Sigma}$ is full row rank. There, $\boldsymbol{\Sigma}^\perp \in \mathbb{R}^{2N\times(2N-2)}$ and $\boldsymbol{\Sigma}^\dagger \in \mathbb{R}^{2N\times 2}$ which fulfill $\boldsymbol{\Sigma}\boldsymbol{\Sigma}^\perp = \boldsymbol{0}$ and $\boldsymbol{\Sigma}\boldsymbol{\Sigma}^\dagger = \boldsymbol{I}$ respectively are defined. In addition, $\tilde{\boldsymbol{U}}$ is obtained by

$$\boldsymbol{U} := [\boldsymbol{\Sigma}^\dagger \quad \boldsymbol{\Sigma}^\perp]\tilde{\boldsymbol{U}}. \tag{34}$$

By assigning (34) to (20), $\boldsymbol{Y} = [\boldsymbol{I} \quad \boldsymbol{0}]\tilde{\boldsymbol{U}}$ is given. Therefore, $\tilde{\boldsymbol{U}}$ is represented by

$$\tilde{\boldsymbol{U}} = \begin{bmatrix}\boldsymbol{Y} & \boldsymbol{q}\end{bmatrix}^T, \tag{35}$$

where $\boldsymbol{q} \in \mathbb{R}^{(2N-2)\times 1}$ is a free parameter.

By substituting (29), (34), and (35) to (26), the evaluation function J is transformed as follows:

$$J = R(\boldsymbol{q}) + \boldsymbol{S}^T(\boldsymbol{q})\boldsymbol{Q}\boldsymbol{S}(\boldsymbol{q}), \tag{36}$$

$$\boldsymbol{Z} := \boldsymbol{I}^* - \boldsymbol{A}\boldsymbol{x}[0] - \boldsymbol{B}\boldsymbol{\Sigma}^\dagger\boldsymbol{Y} - \boldsymbol{B}_2\boldsymbol{U}_{EMF}, \tag{37}$$

$$R(\boldsymbol{q}) := \boldsymbol{Z}^T\boldsymbol{Q}\boldsymbol{Z} - 2\boldsymbol{Z}^T\boldsymbol{Q}\boldsymbol{S}(\boldsymbol{q}), \tag{38}$$

$$\boldsymbol{S}(\boldsymbol{q}) := \boldsymbol{B}\boldsymbol{\Sigma}^\perp\boldsymbol{q}. \tag{39}$$

With LMI, the condition which satisfies $J < \gamma$ for provided γ is given by (40) [9].

$$\begin{bmatrix} \gamma - R(\boldsymbol{q}) & \boldsymbol{S}(\boldsymbol{q})^T \\ \boldsymbol{S}(\boldsymbol{q}) & \boldsymbol{Q}^{-1} \end{bmatrix} > 0. \tag{40}$$

Next, the voltage limit is described with LMI. The voltage limits at each sampling point are described as

$$\begin{aligned} \Delta \boldsymbol{T}^T[k]\Delta \boldsymbol{T}[k] &= \Delta T_d^2[k] + \Delta T_q^2[k] \\ &\leq \Delta T_{\max}^2 \ \ (k = 0, 1, \cdots, N-1). \end{aligned} \tag{41}$$

Here, $\boldsymbol{g}(i) \in \mathbb{R}^{2\times 2N}$ $(i := 2k+1)$ of which (1, i) th and (2, $i+1$) th entries are 1 and other entries are 0 is defined. $\boldsymbol{g}(i)$ separates input vector $\Delta \boldsymbol{T}[k]$ as follows:

$$\Delta \boldsymbol{T}[k] = \boldsymbol{g}(i)\boldsymbol{U}(\boldsymbol{q}). \tag{42}$$

With $\boldsymbol{g}(i)$, (41) is transformed as

$$\{\boldsymbol{g}(i)\boldsymbol{U}(\boldsymbol{q})\}^T \{\boldsymbol{g}(i)\boldsymbol{U}(\boldsymbol{q})\} \leq \Delta T_{\max}^2. \tag{43}$$

(43) is expressed with N LMIs by

$$\begin{bmatrix} \Delta T_{\max}^2 & \boldsymbol{U}(\boldsymbol{q})^T \boldsymbol{g}(i)^T \\ \boldsymbol{g}(i)\boldsymbol{U}(\boldsymbol{q}) & \boldsymbol{I} \end{bmatrix} \geq 0, \tag{44}$$

where $i = 2k+1$, $k = 0, 1, \cdots, N-1$.

By minimizing γ under (40) and (44), the FF input, which drives an initial state $\boldsymbol{x}[0]$ to a final state $\boldsymbol{x}[N]$ by the prescribed time interval N for the PWM hold model of SPMSM and minimizes the square sum of current error to fulfill the voltage limit, is obtained.

2) Propsoed method 2: Proposed method 1 can be caused inverse response of q-axis current because q-axis current response is untrammeled. Generally, inverse response of q-axis current is not desirable, so constraint functions of q-axis current response are added in proposed method 2.

$\boldsymbol{f}(i) \in \mathbb{R}^{1\times 2N}$ $(i := 2k+1)$ of which (1, $i+1$) th entry is 1 and other entries are 0 is defined. $i_q[k+1]$ is described with $\boldsymbol{f}(i)$ as follows:

$$i_q[k+1] = \boldsymbol{f}(i)\left(\boldsymbol{A}\boldsymbol{x}[0] + \boldsymbol{B}\boldsymbol{U} + \boldsymbol{B}_2\boldsymbol{U}_{EMF}\right). \tag{45}$$

Therefore, the constraint function which wraps inverse response of q-axis current is represented by

$$\boldsymbol{f}(i)\left(\boldsymbol{A}\boldsymbol{x}[0] + \boldsymbol{B}\boldsymbol{U} + \boldsymbol{B}_2\boldsymbol{U}_{EMF}\right) - i_q[0] \geq 0. \tag{46}$$

By minimizing γ under (40), (44), and (46), the FSC input which drives an initial state $\boldsymbol{x}[0]$ to a final state $\boldsymbol{x}[N]$ by the prescribed time interval N for the PWM hold model of SPMSM, minimizes the square sum of current error to fulfill the voltage limit, and prevent inverse response of q-axis current is obtained.

Here, the FSC input exists in proposed method 2 because it is assumed that ω_e is constant in this paper. However, if speed increases during prescribed time interval, FSC input of proposed method 2 could not exist.

TABLE I
PMSM PARAMETERS

Inductance L	1.80 [mH]
Resistance R	0.157 [Ω]
Pairs of poles P	4
Back EMF constant K_e	74.6 [mV/(rad/s)]

IV. Simulation

The parameters of SPMSM for the simulation are shown in Table I. The dc-bus voltage of the three-phase inverter V_{dc} is 36 [V]. The control period T_u is 0.1 [ms].

Fig. 5 shows simulation results when step torque reference was given and the rotor velocity was 1000 [rpm]. Here, the voltage amplitude of current reference generator was set to be $0.98V_{\max}$. The dq-axis ON time vector amplitude ΔT_a and the dq-axis ON time vector phase (voltage phase) δ are represented by

$$\Delta T_a = \sqrt{\Delta T_d^2 + \Delta T_q^2}, \tag{47}$$

$$\delta = \tan^{-1}\frac{-\Delta T_d}{\Delta T_q}. \tag{48}$$

The dotted lines in Fig. 5(c), 5(g), and 5(k) are described $\Delta T_{\max}$.

Conventional method cannot operate the voltage phase because it consists of current vector control. Therefore, the voltage phase variation was slow and quick response was not achieved. In addition, when the voltage amplitude was not limited, current response still is slow because anti-windup control made closed-loop discontinuous and conventional method is only composed with FB controllers.

In the proposed method 1 and 2, the FSC inputs were generated as $\boldsymbol{Q} = \boldsymbol{I}$. The prescribed time interval N was chosen to be the quickest response (proposed method 1: $N = 40$, proposed method 2: $N = 49$). During the beginning of transient response, inverse reponse of q-axis current happened but d-axis current variation is large. This made large d-axis current quickly. Finally, proposed method 1 achieved the quickest response. On the other hand, proposed method 2 suppressed inverse respose of q-axis current and maximum overshoot. However, the settling time is larger than one of proposed method 2.

V. Experiment

Experimental results are shown in Fig. 6. Experiments were performed in the same condition as simulations. The parameters of SPMSM and the control period were the same too. The load motor which controled velocity was the same with the controlled motor. Therefore, for quick current control of load motor, V_{dc} was set to be 80 [V]. In the controller calculation, the nominal three-phase inverter dc-bus voltage was $V_{dcn} = 36$ [V] and the input was multiplied by V_{dcn}/V_{dc} to compensate the difference between V_{dc} and V_{dcn} in SVM. $\Delta\theta$ in experiments is $0.9\omega_e T_u$ to consider the computational time $0.4T_u$.

The variations of d-axis reference in all experimental results are due to speed variation. In conventional method,

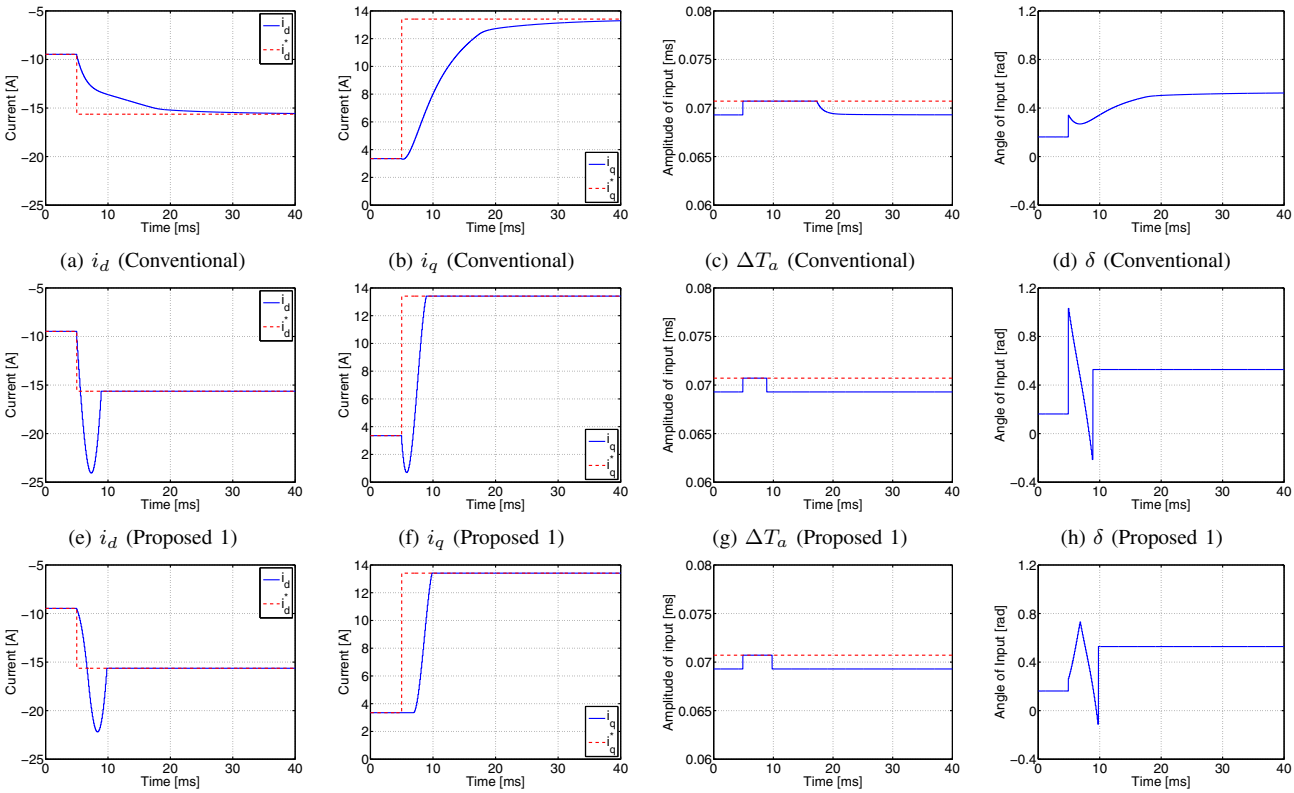

(a) i_d (Conventional) (b) i_q (Conventional) (c) ΔT_a (Conventional) (d) δ (Conventional)

(e) i_d (Proposed 1) (f) i_q (Proposed 1) (g) ΔT_a (Proposed 1) (h) δ (Proposed 1)

(i) i_d (Proposed 2) (j) i_q (Proposed 2) (k) ΔT_a (Proposed 2) (l) δ (Proposed 2)

Fig. 5. Simulation result (Proposed 1: $N = 40$, Propsoed 2: $N = 49$)

the voltage phase variation was slow and anti-windup control deteriorated current response.

In the proposed methods, the FSC inputs which are the same as simulations were calculated by off-line. When torque reference was obtained, the FF inputs were output from time series table of FSC input. If the response is not settled during the prescribed time interval, the FF input was generated from (19). Proposed method 1 achieved the quickest response. current is not settled during prescribed time interval because of speed variation. The q-axis current response of proposed method 2 is slower than one of proposed method 1 but proposed method 2 improved undershoot of q-axis current and maximum overshoot of d-axis current.

VI. Analysis Current Response Using Voltage Limit Circle with Transient Term

This section expresses the voltage limit circle with transient term for SPMSM. In addition, the FSC inputs of both proposed methods are analyzed by using it.

A. Voltage limit circle with transient term

The dq-axis voltage equation which is represented by (1) is described under voltage limit ($v_d^2+v_q^2 \leq V_{\max}^2$) as follows:

$$\left(\frac{V_{\max}}{L}\right)^2 \geq \left(\dot{i}_d - C_d\right)^2 + \left(\dot{i}_q - C_q\right)^2, \tag{49}$$

(50)

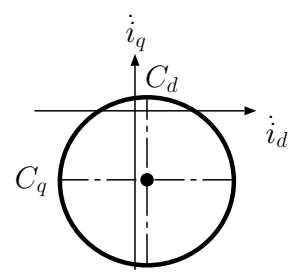

Fig. 7. Voltage limit circle with transient term ($\omega_e \geq 0$, powering)

$$C_d = -\frac{R}{L} i_d + \omega_e i_q, \tag{51}$$

$$C_q = -\omega_e i_d - \frac{R}{L} i_q - \frac{\omega_e K_e}{L}. \tag{52}$$

This is the voltage limit circle with transient term. Here, C_d and C_q are the d-axis and q-axis center coordinates of the voltage limit circle with transient term, respectively. In general, the voltage limit circle of SPMSM represents d-axis and q-axis current under voltage limit. The voltage limit circle with transient term expresses d-axis and q-axis current variation $\dot{i}_d$ and $\dot{i}_q$ under voltage limit.

B. Current response of SPMSM under voltage limit

$C_d \geq 0$ and $C_q \leq 0$ when $\omega_e \geq 0$ and the SPMSM is powering. Therefore, the center of voltage limit circle with transient term exists on fourth quadrant as shown in Fig. 7.

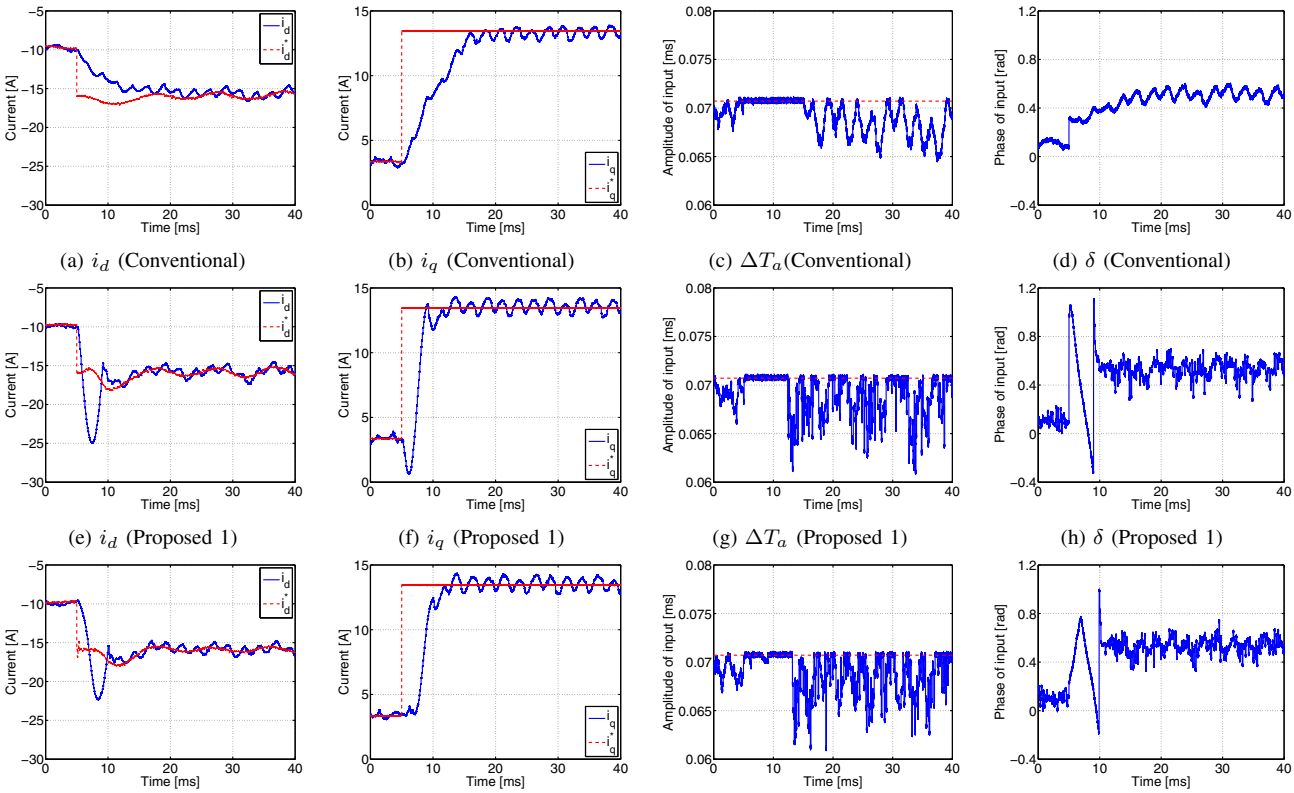

(a) i_d (Conventional) (b) i_q (Conventional) (c) ΔT_a(Conventional) (d) δ (Conventional)

(e) i_d (Proposed 1) (f) i_q (Proposed 1) (g) ΔT_a (Proposed 1) (h) δ (Proposed 1)

(i) i_d (Proposed 2) (j) i_q (Proposed 2) (k) ΔT_a (Proposed 2) (l) δ (Proposed 2)

Fig. 6. Experimental result (Proposed 1: $N = 40$, Propsoed 2: $N = 49$)

Here, the area on fourth quadrant ($\dot{i}_d \geq 0$, $\dot{i}_q \leq 0$) is large, so quick response as $\dot{i}_q \leq 0$ can be achieved easily. On the other hand, quick response as $\dot{i}_q \geq 0$ is not expected because the area on second quadrant ($\dot{i}_d \leq 0$, $\dot{i}_q \geq 0$) is small. That is to say the operation which extends the area on second quadrant is necessary.

Here, center coordinates C_d, C_q are partially differentiated by $-i_d$, i_q as follows:

$$\frac{\partial C_d}{\partial(-i_d)} = \frac{R}{L}, \quad \frac{\partial C_q}{\partial(-i_d)} = \omega_e, \tag{53}$$

$$\frac{\partial C_d}{\partial i_q} = \omega_e, \quad \frac{\partial C_q}{\partial i_q} = -\frac{R}{L}. \tag{54}$$

This mentions that the center of voltage limit circle with transient term is moved to fist coordinate and fourth coordinate by $\dot{i}_d < 0$ and $\dot{i}_q > 0$, respectively. Especially, in high-speed operation, the variations of C_d and C_q are subject to $\dot{i}_q$ and $\dot{i}_d$, respectively, because of $\omega_e \gg \frac{R}{L}$ as shown in Fig. 8.

Namely, large $\dot{i}_q > 0$ is undesirable at beginning of transient response because it decreases the area on second coordinate. On the other hand, $\dot{i}_d < 0$ increases the area on second coordinate. If d-axis current is preferentially flowed at beginning of transient response, q-axis current response can be improved. Moreover, if inverse response of q-axis current is acceptable, a point on third coordinate ($\dot{i}_d \leq 0$, $\dot{i}_q \leq 0$) can be selected. The point of maximum d-axis current variation exists on third coordinate. In addition, if d-axis current is

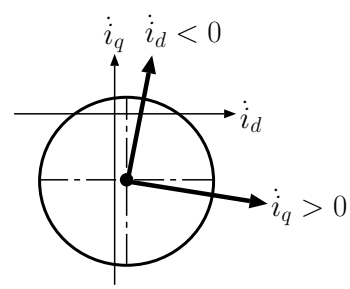

Fig. 8. Transit of voltage limit circle with transient term on high-speed operation ($\omega_e \geq 0$, powering)

negatively larger than d-axis current reference, a point on first coordinate ($\dot{i}_d \geq 0$, $\dot{i}_q \geq 0$) can be taken. Thus, quick q-axis response is prospected because there is a point of maximum $\dot{i}_q$. By the aforementioned process, quickest current response is realized.

Fig. 9 shows the transit of voltage limit circle with transient term in simulation. Conventional method selected a point on second coordinate only. Therefore, the area on second coordinate decreased and q-axis current response is deteriorated. In order to improve q-axis current variation, proposed method 1 moves the center of voltage limit circle to the second coordinate by q-axis current undershoot and d-axis current overshoot and achieve the quickest response. Proposed method 2 does not change q-axis current but d-axis

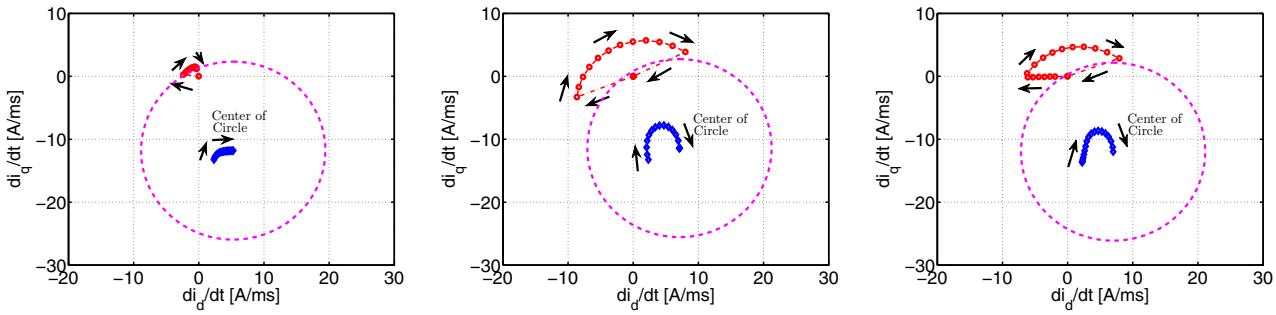

(a) Conventional method (b) Proposed method 1 (c) Proposed method 2

Fig. 9. Transit of voltage limit circle with transient term (simulation)

current at beginning of transient response. Thus, the center of voltage limit circle is moved to the first coordinate and it increases the area on second coordinate. However, d-axis current variation is negatively smaller than one of proposed method 2 because q-axis current undershoot does not happen. This mentions that changing q-axis current decreases the settling time better than increasing d-axis current overshoot. Therefore, maximum d-axis current overshoot decreases.

The reason why proposed methods can act these operations is because they use PWM hold model and consider voltage limit.

VII. Conclusion

For quick current response under voltage limit, our previous paper proposed final-state control considering voltage limit but inverse response of q-axis current happened. This paper proposes a new FSC input which suppresses inverse response of q-axis current. Simulations and Experiments are performed to show that proposed method 2 can suppress maximum d-axis current overshoot and q-axis current undershoot. However, the settling time of proposed method 2 is longer than one of proposed method 1. This reason is explained by using voltage limit circle with transient term. In short, our proposed methods consider voltage limit circle with transient term exactly.

In our future work, online calculation of proposed methods will be realized and robust feedback controller for modeling error is worked out.

References

[1] B.-H. Bae and S.-K. Sul: "A Novel Dynamic Overmodulation Strategy for Fast Torque Control of High-Saliency-Ratio AC Motor", IEEE Trans. Ind. Appl., Vol.41, No.4, pp.1013–1019, 2005.

[2] S. Lerdudomsak, S. Doki, and S. Okuma: "Voltage Limiter Calculation Method for Fast Torque Response of IPMSM in Overmodulation Range", The 35th Annual Conference of the IEEE Industrial Electronics Society, pp. 1385–1390, 2009.

[3] K. Kondo, K. Matsuoka, Y. Nakazawa, and H. Shimizu: "Torque feedback control for salient pole permanent magnet synchronous motor at weakening flux control range", IEEJ Trans. IA, Vol.119, No.10, pp.1155–1164, 1999 (in Japanese).

[4] T.-S. Kwon, G.-Y. Choi, M.-S. Kwak, and S.-K Sul : "Novel Flux-Weakening Control of an IPMSM for Quasi-Six-Step Operation", IEEE Trans. Ind. Appl., Vol.44, NO.6, pp.1722–1723, 2008.

[5] H. Nakai, H. Ohtani, E. Satoh, and Y. Inaguma: "Development and Testing of the Torque Control for the Permanent-Magnet Synchronous Motor", IEEE Trans. Ind. Electron., Vol.52, No.3, pp.800–806, 2005.

[6] W. Hatsuse, Y. Notohara, K. Ohi, K. Tobari, K. Tamura, C. Unoko, and Y. Iwaji: "A Stable Field-Weakening Control Using Voltage Phase Operations in the High-Power Region", The 2010 International Power Electronics Conference, pp.599–604, 2010.

[7] T. Totani and H. Nishimura: "Final-State Control Using Compensation Input", Trans. of the SICE, Vol.30, No.3, pp.253–260, 1994.

[8] T. Miyajima, H. Fujimoto, and M. Fujitsuna: "Field-Weakening Control for SPMSM Based on Final-State Control Considering Voltage Limit", 8th International Conference on Power Electronics, pp.1392–1397, 2011.

[9] M. Hirata, T. Hasegawa, and K. Nonami: "Seek Control of Hard Disk Drives Based on Final-State Control Tracking Account of the Frequency Compensates and the Magnitude of Control Input", The 7th International Workshop on Advanced Motion Control, pp.40–46, 2002.

[10] S. Boyd, L. E. Ghaoui, E. Feron, and V. Balakrishnan: "Linear Matrix Inequalities in System and Control Theory", Society for Industrial and Applied Mathematics, 1994.

[11] K. P. Gokhale, A. Kawamura, and R. G. Hoft: "Deat beat microprocessor control of PWM inverter for sinusoidal output waveform synthesis", IEEE Trans. Ind. Appl., Vol.23, No.3, pp.901–910, 1987.

[12] K. Sakata and H. Fujimoto: "Perfect Tracking Control of Servo Motor Based on Precise Model with PWM Hold and Current Loop", The Forth Power Conversion Conference, pp.1612–1617, 2007.

[13] J. Kudo, T. Noguchi, M. Kawakami, and K. Sano: "Mathematical Model Errors and Their Compensations of IPM Motor Control System", IEE of Japan Technical Meeting Record, IEE Japan, SPC-08-25, pp.25–31, 2008 (in Japanese).